High-lying resonances observed in heavy-ion transfer reactions

G. H. Yoo, G. M. Crawley, N. A. Orr, and J. S. Winfield
National Superconducting Cyclotron Laboratory and Department of Physics and Astronomy, Michigan State University, East Lansing, Michigan 48824

J. E. Finck
Physics Department, Central Michigan University, Mt. Pleasant, Michigan 48859

S. Gales, Ph. Chomaz, I. Lhenry, and T. Suomijärvi
Institut de Physique Nucleaire, F91406 Orsay, France
(Received 10 August 1992)

High-lying single-particle and single-hole states were studied using (^{7}Li,^{6}Li), (^{7}Li,^{6}He), (^{12}C,^{13}C), and (^{12}C,^{13}N) reactions at 30 MeV/nucleon on the targets ^{207}Pb, ^{208}Pb, ^{209}Bi, ^{89}Y, ^{90}Zr, and ^{91}Zr. Broad resonancelike features were observed in both proton and neutron transfer reactions at excitation energies close to the excitation energies of the giant quadrupole resonances. The measured excitation energies and reaction Q values suggest that these features are predominantly single-particle states rather than collective giant resonance excitations. The existence of an extra particle or hole outside closed-shell nuclei does not change the strengths of the broad peaks significantly, but does change the excitation energies in some cases. Shell model calculations in the Pb region support this conclusion.
PACS number(s): 25.70.Hi

I. INTRODUCTION

Broad resonancelike structures have been observed in a number of single-particle transfer reactions [1], particularly with heavy-ion projectiles [2–5]. They have been interpreted as arising from the transfer of a nucleon into a high (or a deep-lying) orbit, in agreement with the deduced characteristics (energy, width, strength) of the given structures [1, 6, 7]. However, the fact that in some cases these broad peaks have excitation energies and widths consistent with known giant resonance states has led some authors [8] to propose that these features could be associated with collective excitations of some kind, in spite of the fact that they are observed in single-particle transfer reactions. The situation is complicated, particularly in stripping reactions, by the underlying background which makes it difficult to extract the position and strength of the resonances accurately. This background has not yet been quantitatively explained. The present paper will discuss measurements intended to help explain the origin of these resonancelike features.

As will be shown in more detail in Sec. II, the two different explanations for the resonancelike bumps lead to different predictions for the positions and strengths of peaks observed on the same single-nucleon transfer reactions on adjacent even-even and odd-even nuclei. To check these predictions, single-neutron and single-proton transfer reactions were carried out on targets of ^{89}Y, ^{90}Zr, ^{91}Zr, ^{207}Pb, ^{208}Pb and ^{209}Bi using beams of ^{7}Li and ^{12}C from the K500 cyclotron at Michigan State University. These projectiles were chosen mainly because the resonancelike structures appear particularly pronounced for heavy projectiles [3, 5] and to reduce the ejectile excitation problem discussed below. In order to exclude differences in the spectra arising from different kinematic conditions, all reactions on neighboring targets were carried out under identical experimental conditions with the same beam, the same bombarding energy, and the same scattering angle. These constraints allow meaningful comparisons between the experimental spectra on different targets.

Two problems often encountered in heavy-ion transfer reactions need to be addressed. The first is ejectile excitation. The nuclear species emitted following the transfer reaction may be excited as well as the residual nucleus consisting of target plus particle or hole. Excitation of states in the ejectile may give rise to peaks in the spectrum of emitted particles which could be misidentified as states in the final nucleus. This problem can be minimized by choosing cases where the ejectile has a low threshold for particle emission. Once the ejectile is excited above the particle threshold, it breaks up before it can be detected. In the present experiment, ^{6}He, ^{6}Li, and ^{13}N have no particle stable states. Thus these ejectiles cannot give rise to spurious peaks in the residual nucleus spectrum. The other cases of ^{11}C, ^{13}C, and ^{11}B ejectiles following single-particle transfer reactions with a ^{12}C beam do not fit this criterion well and so were not studied extensively.

The other problem, particularly for stripping reactions, is the large background underlying the resonancelike structure. This background is believed to arise, at least partly, from the breakup of the projectile leading to continuum states. The nature of this background is

a long standing problem which will not be addressed extensively in this paper, since elucidation of the origin of the background probably requires coincidence measurements.

II. MODELS FOR THE EXCITATION PROCESS

The two alternative descriptions of these states lead to somewhat different predictions for their excitation energy and strength when the same reaction is carried out on neighboring even-even and odd-even targets.

A. Single-particle excitations

The single-particle explanation of these broad high-lying structures assumes that these states are formed, as are the low-lying states, by transfer of a single particle (stripping) or the production of a single hole (pickup) in a one-step process. The states formed are broad because the single-particle states are unbound and mix with the more complex underlying states. The peaks stand out in some reactions above the background because the kinematic conditions favor states of high spin, which are then preferentially excited compared to the underlying low-spin states.

If the broad resonancelike peaks are single-particle excitations, they should appear in the spectra of neighboring targets with one particle added or subtracted from the even-even core. There may be some shift in the excitation energy and a slight broadening of the peak because of the extra particle or hole, but the total strength should be very similar for the same reaction on targets in the same mass region. For example, consider a neutron stripping reaction on the even-even nucleus ^{208}Pb leading to the residual nucleus ^{209}Pb. The low-lying states formed by such a reaction in ^{209}Pb are the well-known single-neutron states ($2g_{9/2}$, $1i_{11/2}$, and $1j_{15/2}$) above the closed $N = 126$ core. If the same reaction is carried out on the neighboring odd-even nucleus ^{209}Bi, which has an $1h_{9/2}$ proton outside the closed $Z = 82$ core, multiplets of states are formed from the coupling of the $1h_{9/2}$ proton with the neutron states. These multiplets occur at very similar excitation energies in ^{210}Bi as the single-neutron states in ^{209}Pb. However, a slightly different situation arises if a ^{207}Pb target is used. In this case, the target has a single, predominantly $p_{1/2}$ neutron hole in the closed $N = 126$ shell. Therefore the ground state of ^{208}Pb would be formed by filling this hole. This is highly improbable in transfer reactions using heavy ions, and therefore the ground state will be only weakly populated. Conversely, the cross section for transferring a neutron to a single-particle orbital will be independent of the presence of a hole in the Pb core, and therefore one expects to observe the same peaks as in the reaction on the even-even target. The only differences will be that the coupling with the preexisting hole will generate a multiplet of different spins and will shift the peaks by the energy of the hole state. This shift is approximately the energy difference between the 0^+ ground state and the energy of the hole state. In the case of the ^{207}Pb target, this energy difference is about 3.4 MeV.

Shell model calculations will be described in the next section which supports this observation. These observations are general properties of single-particle transfer reactions on neighboring nuclei. Since the small shifts in excitation energy are caused by particle-particle and particle-hole interactions and do not depend very critically on spin, similar behavior is to be expected also at high excitation energy. An analogous situation arises for pickup reactions. Measurements which illustrate these points have been made with good resolution where the individual members of the multiplets can be resolved in the low-lying regions of ^{206}Pb and ^{208}Bi [9, 10].

In conclusion, a clear signature of single-particle states is the observation of a shift in excitation energy of corresponding states in neighboring nuclei both when the final nucleus is a closed-shell nucleus and when two identical particles are placed in the same orbit in the final nucleus.

B. Collective excitations

The excitation of collective states by transfer reactions has already been used in the past to study the structure of low-lying states [11]. The idea is simple to understand when one starts with a target which consists of a single-hole (-particle) state and then transfers a particle (hole). In this case, the result is a particle-hole excitation of the closed-shell nucleus which will have some overlap with the collective states. Indeed, in a microscopic description, these collective states correspond to a coherent sum of particle-hole configurations. In principle, the cross section expected for excitation of these collective states will be small because the coherence is lost when exciting only one configuration. However, it has been proposed recently that this coherence can be partly recovered if the reaction excites several configurations at the same time [8]. In this case, the cross section for exciting giant resonances may become comparable to or even greater than the cross section for exciting single-particle (-hole) states. This would be of great importance because the particle transfer process can be thought of as the inverse of the direct particle decay to the ground state. Therefore, within the detailed balance hypothesis, it would be possible to compare the two observations and to obtain information on the microscopic structure of giant resonances in nuclei.

The discussion above considered the case where the final nucleus is a closed-shell nucleus. In other cases, with non-closed-shell final nuclei, the same concepts apply, but the quantitative discussion is more complicated because of the need to have a good microscopic description of the particle-hole correlations in the ground state of even-even nuclei.

To summarize, giant resonances may be excited in transfer reactions. Their cross section, however, should vary dramatically depending on the structure of the target ground state, on the matching conditions, and on the number of accessible configurations which can be coupled. Moreover, a rather smooth dependence of the excitation energies of such structures is expected. Indeed, giant resonances are a general property of all nuclei and

their excitation energies depend weakly on the nuclear structure. Therefore, only small variations in excitation energies are expected in neighboring nuclei even though different resonances can be excited with different targets, projectiles, and incident energies. These expectations contrast strongly with the behavior expected for the case of single-particle excitations.

III. EXPERIMENTAL METHOD

The transfer reactions (^{7}Li,^{6}Li), (^{7}Li,^{6}He), (^{12}C,^{13}C), and (^{12}C,^{13}N) were carried out at a bombarding energy of 30 MeV/nucleon using beams from the K500 superconducting cyclotron at Michigan State University. The reaction products were momentum analyzed with the S320 broad range magnetic spectrograph [12] and detected by the focal plane detector system. In each reaction, the ejectiles were measured at the grazing angles to maximize the cross sections. The energy resolution was about 500 keV full width at half maximum (FWHM) for the ^{6}Li and ^{6}He spectra, and about 1 MeV FWHM for the ^{12}C, ^{13}C, and ^{13}N spectra. Six self-supporting metal foil targets, ^{89}Y (5.30 mg/cm^2, 100%), ^{90}Zr (5.06 mg/cm^2, 97.62%), ^{91}Zr (5.01 mg/cm^2, 88.5%), ^{207}Pb (4.95 mg/cm^2, 92.40%), ^{208}Pb (5.84 mg/cm^2, 99.14%), and ^{209}Bi (6.50 mg/cm^2, 100%), were used in this experiment.

The focal plane detector consisted of three modular units: position sensitive counters, ion chambers, and scintillators. Depending on the charges and the energies of the reaction products, different types of gases and pressures were used. For the ^{12}C beam, 100% isobutane gas was used at 70 torr, and for the ^{7}Li beam, a mixture of 20% of isobutane gas and 80% of freon gas was used at 140 torr. The particle identification was done with two contours on the energy loss versus total energy and time of flight versus position spectra. Because the counting rate of elastically scattered ^{12}C particles was much larger than that of ^{13}C particles, the ^{12}C particles in the (^{12}C,^{13}C) reactions studied were blocked by using a narrow metal post or "finger."

The energy calibration of the focal plane for the (^{7}Li,^{6}Li) and (^{7}Li,^{6}He) reactions was obtained using a ^{12}C target and observing known states in ^{13}C and ^{13}N. To minimize the uncertainty due to the energy loss in the target, a very thin ^{12}C target (0.48 mg/cm^2) was used. For the calibration of the neutron and proton pickup reactions (^{12}C,^{13}C) and (^{12}C,^{13}N), the elastic scattered particles from ^{12}C and ^{90}Zr were moved across the focal plane by varying the magnetic field of the dipole. The uncertainty of the calibration was about 0.15 MeV for ^{6}Li and ^{6}He, and about 0.3 MeV for ^{13}C and ^{13}N. The main uncertainties arose from the measurement of the thickness of the target and the determination of the position of the peaks on the focal plane.

IV. SHELL MODEL CALCULATIONS

In single-nucleon transfer reactions on targets which have an extra hole or particle outside a closed shell, the interaction between the transferred nucleon and the target's hole or particle splits the single-particle states and produces a multiplet of states. Shell model calculations have successfully predicted properties of these states in the vicinity of closed-shell nuclei, especially in the lead region [13–16].

In the present work, shell model calculations were performed for two target nuclei: ^{207}Pb and ^{209}Bi. The purpose of the shell model calculations was to observe how the characteristics of single-particle states in the multiplet, such as excitation energies, widths, and spectroscopic factors, are changed by the presence of a single particle or hole outside a closed-shell nucleus.

The shell model calculations were performed with the National Superconducting Cyclotron Laboratory version of the program OXBASH [17]. This code can handle up to three particle orbits and four hole orbits in both proton and neutron shells. The targets were assumed to be a composite of the ^{208}Pb core nucleus and a single-proton particle for the ^{209}Bi nucleus or a single-neutron hole for the ^{207}Pb nucleus. Energetically the highest four hole orbits (proton hole, $1h_{11/2}, 3s_{1/2}$, $2d_{3/2}, 2d_{5/2}$; neutron hole, $1i_{13/2}, 3p_{1/2}$, $3p_{3/2}, 2f_{5/2}$) and the lowest three particle orbits (proton particle, $1h_{9/2}, 2f_{7/2}$, $1i_{13/2}$; neutron particle, $2g_{9/2}, 1i_{11/2}$, $1j_{15/2}$) were considered to be the available particle and hole states [13].

In the ^{207}Pb$(+n)$ reaction, when the transferred neutron occupies one of the three neutron particle states, the neutron hole which is initially in the $3p_{1/2}$ level can occupy any one of the four neutron hole states in the final state, while the proton shell remains closed. [The notation $(+n)$ stands for adding a neutron to the target by a neutron stripping reaction.] As a result, 12 combinations of one-particle–one-hole states were used in the calculations. If the neutron occupies the target's initial hole state $3p_{1/2}^{-1}$, the neutron shell becomes closed. In this case, the proton shell is either closed or a proton can be excited to one of the three proton particle states from one of the proton hole states, making 13 (1+12) combinations. Thus, a total of 25 combinations of particle and hole states were considered. The same procedures were also used for the other reactions. In the ^{209}Bi$(+n)$ reaction, since the target nucleus has a proton in the $1h_{9/2}$ orbit, the main interaction is between the transferred neutron and an outermost shell's proton.

The results of the shell model calculations for the energy levels are expressed as an excitation energy, spectroscopic factor S, j^{π} of the residual nucleus, and the transferred nucleon's final orbit quantum numbers n, l, and j. The cross section σ_f is defined as

$$\sigma_f = \sigma_{\rm th} \frac{2j_f + 1}{2j_i + 1} S_f, \tag{1}$$

where $\sigma_{\rm th}$ is the calculated cross section which takes account of the kinematics and distortion effects and may be assumed to be constant for the same orbit, j_f and j_i are the total angular momentum of the final and initial states, respectively, and S_f is the spectroscopic factor of the final state. The single-particle states in the ^{209}Pb and ^{209}Bi nuclei were independently normalized to the experi-

TABLE I. Average excitation energies obtained using shell model calculations for three peaks from proton stripping reactions on targets of ^{207}Pb and ^{209}Bi are shown with the experimental data. The values in parentheses are the reaction Q values for the corresponding excitation energies. Energies of the single-particle states from the ^{208}Pb(+p) reaction are also given to measure the energy shift due to the particle-particle or particle-hole interactions. Experimental errors are about 0.15 MeV.

	Single state	Shell model calculations		This experiment (^{7}Li ,^{6}He)	
Peak	^{208}Pb(+p)	^{207}Pb(+p)	^{209}Bi(+p)	^{207}Pb(+p)	^{209}Bi(+p)
1	0.	0.098	1.479	0.03	1.39
	(−6.716)	(−6.366)	(−6.270)	(−6.27)	(−6.38)
	$\pi(h_{9/2})$	$\nu(p_{1/2})^{-1} \otimes \pi(h_{9/2})$	$\pi(h_{9/2}) \otimes \pi(h_{9/2})$		
2	0.897	1.134	2.354	0.90	2.12
	(−7.073)	(−7.402)	(−7.324)	(−7.17)	(−7.11)
	$\pi(f_{7/2})$	$\nu(p_{1/2})^{-1} \otimes \pi(f_{7/2})$	$\pi(h_{9/2}) \otimes \pi(f_{7/2})$		
3	1.609	1.718	3.002	1.52	2.73
	(−7.715)	(−7.987)	(−7.980)	(−7.79)	(−7.72)
	$\pi(i_{13/2})$	$\nu(p_{1/2})^{-1} \otimes \pi(i_{13/2})$	$\pi(h_{9/2}) \otimes \pi(i_{13/2})$		

mental data. The average energies of each multiplet were obtained by averaging the energies weighted by the cross section. They are compared with the present experimental data, and the centroid energies are compared with the single-particle states of the ^{209}Pb and ^{209}Bi nuclei in Tables I and II, and Fig. 1.

In the ^{207}Pb(+n) reaction, the energy levels except the ground state are shifted to higher excitation, which agrees well with the experimental result. In the ^{209}Bi(+n) reaction, the widths of the multiplets (about 500 keV) are somewhat larger than those (100–300 keV) of the multiplets in the ^{207}Pb(+n) reaction. The reason is that the ground state of ^{209}Bi has a large angular momentum ($1h_{9/2}$) and the coupling with the neutron particle states allows many j_f ranging from $|j - \frac{9}{2}|$ to $j + \frac{9}{2}$. In the ^{207}Pb(+p) reaction, two dominant levels appear in each multiplet. Because of the very weak *odd-odd* coupling strength between the $3p^{-1}_{1/2}$ state of ^{207}Pb and the proton's single-particle states, the widths of the multiplets are about 70 keV and there is about a 0.1 MeV shift of the whole spectrum to higher excitation.

In the ^{209}Bi(+p) reaction, the widths of the multiplets (about 300 keV) are not as large as the widths of the multiplets (about 500 keV) in the ^{209}Bi(+n) reactions. The ground state of the *even-even* residual nucleus ^{210}Po is shifted from the centroid of the $\pi(1h_{9/2})^2$ multiplet to lower energy by 1.38 MeV, because of the pairing interaction in the $\pi(1h_{9/2})^2$ $j = 0^+$ state. This shift is much larger than that of the ground state for the *even-odd* residual nucleus of the ^{209}Bi(+n) reaction, namely, 0.36

TABLE II. Average excitation energies obtained using shell model calculations for three peaks from neutron stripping reactions on targets of ^{207}Pb and ^{209}Bi are shown with the experimental data. The values in parentheses are the reaction Q values for the corresponding excitation. Energies of the single-particle states from the ^{208}Pb(+n) reaction are also given to measure the energy shift due to the particle-particle or particle-hole interactions. Experimental errors are about 0.15 MeV.

	Single state	Shell model calculations		This experiment (^{7}Li, ^{6}Li)	
Peak	^{208}Pb(+n)	^{207}Pb(+n)	^{209}Bi(+n)	^{207}Pb(+n)	^{209}Bi(+n)
1	0.	3.557	0.414	3.30	0.65
	(−3.313)	(−3.400)	(−3.060)	(−3.11)	(−3.30)
	$\nu(g_{9/2})$	$\nu(p_{1/2})^{-1} \otimes \nu(g_{9/2})$	$\pi(h_{9/2}) \otimes \nu(g_{9/2})$		
2	0.779	4.281	1.201	4.14	1.51
	(−4.092)	(−4.164)	(−3.832)	(−4.02)	(−4.16)
	$\nu(i_{11/2})$	$\nu(p_{1/2})^{-1} \otimes \nu(i_{11/2})$	$\pi(h_{9/2}) \otimes \nu(i_{11/2})$		
3	1.423	4.939	1.760	4.70	2.01
	(−4.736)	(−4.712)	(−4.406)	(−4.58)	(−4.66)
	$\nu(j_{15/2})$	$\nu(p_{1/2})^{-1} \otimes \nu(j_{15/2})$	$\pi(h_{9/2}) \otimes \nu(j_{15/2})$		

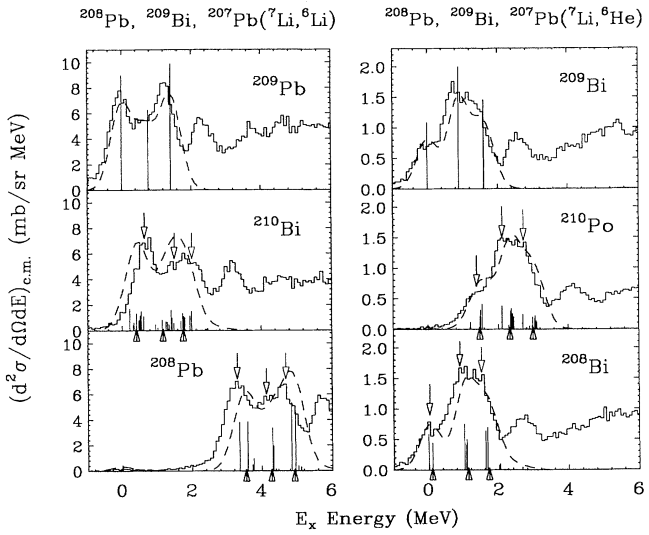

FIG. 1. Comparison of shell model calculations with experimental spectra. The height of each vertical bar represents the strength of a specific configuration, the solid lines are experimental data, and the dashed lines are calculated spectra obtained using a Gaussian distribution with the 0.3 MeV FWHM. Calculated values are normalized to the experimental data. The average excitation energies of the shell model calculations for each multiplet are marked with short arrows on the horizontal axis, while the centroid of experimental peaks are marked with long arrows on the spectra.

MeV.

As is shown in Tables I and II, even though the energy levels in the multiplets are spread up to 4 MeV, the relative excitation energies for the centroid of each multiplet do not differ significantly from those of the single-particle states in the ^{209}Pb or ^{209}Bi nucleus (at most by a few hundred keV). When the reaction Q values of the multiplets are compared with those of the single-particle states, no significant differences are observed. However, when the excitation energies are compared, significant differences are observed in some cases. From these comparisons, it is evident that the existence of an extra hole or particle in the target does not change the reaction Q values significantly, but in certain specific cases the excitation energies may change significantly.

V. RESULTS AND DISCUSSION

For both the stripping and pickup cases, the spectra of the same reactions on neighboring targets were compared. In all cases, the spectra on neighboring targets were very similar and the same broad features were observed with similar strength. However, the excitation energies observed for similar peaks were different for neighboring targets in some cases. The reactions may be divided into two groups which are discussed separately in the following two sections.

A. Final nucleus is a closed core

In four of the reactions considered in this study, the projectile stripping reactions ^{89}Y(^{7}Li,^{6}He)^{90}Zr and ^{207}Pb(^{7}Li,^{6}Li)^{208}Pb and the pickup reactions ^{91}Zr(^{12}C,^{13}C)^{90}Zr and ^{209}Bi(^{12}C,^{13}N)^{208}Pb, the ground state of the final nucleus has both the proton shell and the neutron shell closed.

Energy spectra of the stripping reactions ^{89}Y$(+p)$ and ^{207}Pb$(+n)$ are shown in Fig. 2. The ejectiles were measured at the grazing angle and $E_{\rm inc}$ = 30 MeV/nucleon. In the figure, the dotted lines represent the background and the arrows at the bottom indicate the location of the centroid of the peaks analyzed. The same Gaussian peak shape with the same FWHM was used throughout the analysis. The analyzed peaks are identified by a number, and this same number is used to identify peaks formed by transferring a particle or hole to the same orbit by the same reaction on a neighboring target [e.g., the set of reactions ^{89}Y, ^{90}Zr, ^{91}Zr(^{7}Li,^{6}He)]. A substantial continuum is evident, especially at high excitation. This probably arises from projectile breakup. This background has to be subtracted before the strength of the peaks of interest can be obtained.

The ground states of these two closed-shell final nuclei (labeled as peak number 0) are extremely weak. The ground state of the residual nucleus ^{90}Zr is formed when a transferred proton fills the $2p_{1/2}$ hole state. This transition is very similar to that of the ^{207}Pb$(+n)$ reaction where the ^{208}Pb ground state is formed when a neutron fills the $3p_{1/2}$ hole state. The ground states are weak because these transitions involve a spin-flip process and

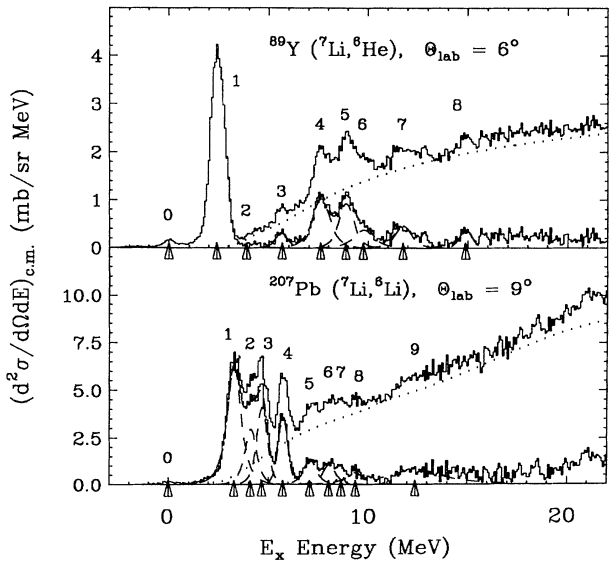

FIG. 2. Energy spectra of the ^{89}Y(^{7}Li,^{6}He) and ^{207}Pb(^{7}Li,^{6}Li) reactions ($E_{\rm inc}$ = 30 MeV/nucleon) which lead to nuclei with closed shells in the ground state (peak 0). The dotted lines indicate the background, and the underlying spectra are obtained after the background is subtracted. Arrows at the bottom in each spectrum represent the centroid of the peaks.

the angular momentum transfer, $1\hbar$ is much smaller than the favored angular momentum transfer $8\hbar$ [18, 19].

In the ^{89}Y$(+p)$ reaction, single-proton particle states couple with the $j = \frac{1}{2}^-$ ground state of ^{89}Y and produce multiplets. Eight excited states were analyzed including a broad state at 11.9 MeV. In the ^{207}Pb$(+n)$ reaction nine excited states were analyzed including a broad state at 13.3 MeV. The first excited state, a composite of 5^- and 4^- states resulting from the couplings between $3p_{1/2}$ and $2g_{9/2}$ states, is 3.30 MeV above the ground state. This energy difference is very similar to the outmost neutron's binding energy difference (3.43 MeV) between the ^{208}Pb and ^{209}Pb nuclei.

The spectra for the (^{7}Li,^{6}He) reaction on the set of neighboring targets ^{90}Zr, ^{91}Zr, and ^{89}Y are shown in Fig. 3. The data are plotted both as a function of the Q value and excitation energy. The excitation energies, widths, and reaction Q values extracted are given in Table III. This table includes three other sets of reactions, with each set containing one of the reactions that results

TABLE III. Excitation energies for the strong, resolved peaks for pickup and stripping reactions on target sets of ^{90}Zr, ^{91}Zr, and ^{89}Y, and ^{208}Pb, ^{209}Bi, and ^{207}Pb. In each set one reaction leads to a nucleus with filled shells in the ground state and these reactions are marked by a *. Γ is a full width at half maximum, Q is the reaction Q value for a corresponding excitation energy, and the units are MeV. The uncertainty is about 0.15 MeV for ^{6}Li and ^{6}He, and about 0.3 MeV for ^{13}C and ^{13}N. Peak 0 is the ground state of the closed-shell nucleus, and it is shifted to lower energy compared to the ground state energy of the non-closed-shell nucleus.

	^{90}Zr(^{7}Li,^{6}He)^{91}Nb			^{91}Zr(^{7}Li,^{6}He)^{92}Nb			^{89}Y(^{7}Li,^{6}He)^{90}Zr*		
Peak	E_x	Γ	$-Q$	E_x	Γ	$-Q$	E_x	Γ	$-Q$
0							0.0	0.8	1.6
1	0.0	0.8	4.8	0.4	1.0	4.5	2.4	0.9	4.0
3	3.1	0.6	7.9	3.5	0.9	7.6	5.8	1.0	7.4
4	4.9	1.2	9.7	5.1	1.2	9.2	7.8	1.3	9.4
5	6.0	0.8	10.8	6.4	1.3	10.4	9.0	1.7	10.6
7	9.1	3.0	13.9	9.4	3.0	13.5	11.9	3.0	13.5
8	11.9	0.6	16.7	12.5	0.8	16.6	15.0	1.2	16.6

	^{208}Pb(^{7}Li,^{6}Li)^{209}Pb			^{209}Bi(^{7}Li,^{6}Li)^{210}Bi			^{207}Pb(^{7}Li,^{6}Li)^{208}Pb*		
Peak	E_x	Γ	$-Q$	E_x	Γ	$-Q$	E_x	Γ	$-Q$
0							0.0	1.2	−0.1
1	0.0	1.1	3.1	0.7	1.0	3.3	3.3	1.0	3.2
2	0.8	0.6	3.9	1.5	0.7	4.1	4.2	0.8	4.1
3	1.3	0.7	4.4	2.0	0.8	4.6	4.7	0.8	4.6
4	2.4	0.7	5.5	3.1	0.8	5.7	5.8	0.7	5.7
9	10.0	5.0	13.13	11.0	5.0	13.6	13.3	5.0	13.2

	^{90}Zr(^{12}C,^{13}C)^{89}Zr			^{91}Zr(^{12}C,^{13}C)^{90}Zr*			^{89}Y(^{12}C,^{13}C)^{88}Y		
Peak	E_x	Γ	$-Q$	E_x	Γ	$-Q$	E_x	Γ	$-Q$
0				0.0	1.0	2.3			
1	0.0	2.0	7.0	4.2	2.0	6.5	0.0	2.0	6.5
2	4.1	3.5	11.1	8.8	3.5	11.1	4.1	3.5	10.6
4	13.5		20.5	18.0		20.3	13.7		20.2

	^{208}Pb(^{12}C,^{13}N)^{207}Tl			^{209}Bi(^{12}C,^{13}N)^{208}Pb*			^{207}Pb(^{12}C,^{13}N)^{206}Tl		
Peak	E_x	Γ	$-Q$	E_x	Γ	$-Q$	E_x	Γ	$-Q$
0				0.0	1.0	1.9			
1	1.1	3.0	7.2	5.0	3.0	6.9	1.4	3.0	7.0
2	5.4	4.0	11.5	8.3	4.0	10.2	5.7	4.0	11.3
3	17.5	8.0	23.6	18.5	4.0	20.4	18.0	8.0	23.6

in a final nucleus with a closed shell as discussed above.

The spectra in Fig. 3 have very similar structure overall. There is a strong peak (peak 1 in Table III) at low excitation energy and a smaller broad peak (peak 7) at higher excitation energy visible in all three cases. The overall strength of the peaks in all three spectra is quite similar. This indicates that the coupling of the single-proton particle states with the ground state of the target does not significantly change the strength of the high-lying broad states, or the positions of the identified peaks plotted versus reaction Q value. The differences in reaction Q value ranged from 0.0 to 0.8 MeV for the peaks in the ^{90}Zr, ^{91}Zr, and ^{89}Y$(+p)$ reactions. However, there is a significant shift in the excitation energy. As can be seen in Table III and Fig. 3, the low-lying and broad high excitation states of the final nucleus ^{90}Zr, which has both shells closed in the ground state, are shifted to higher excitation than corresponding states in ^{91}Nb and ^{92}Nb by 2.0–3.1 MeV, respectively. This result is similar to the predictions of the shell model calculations made in the lead region and described in Sec. III above.

A similar situation arises in the neutron stripping reactions in the Pb region, viz., ^{207}Pb, ^{208}Pb, and ^{209}Bi $(+n)$. However, in this case the strong peak previously observed near 10 MeV in the ^{208}Pb(^{20}Ne,^{19}Ne) reaction [2] is less strongly excited (see peak 9 in Fig. 2). As seen in Table III, the Q values for corresponding peaks are all within a few hundred keV of each other. But the excitation energy of peak 9 changes from 10.0 MeV in ^{209}Pb to 13.3 MeV in ^{208}Pb. Similar results are observed in the (^{20}Ne,^{19}Ne) reaction on these same targets [4, 5].

Energy spectra of the pickup reactions ^{91}Zr$(-n)$ and ^{209}Bi$(-p)$ are shown in Fig. 4. In both reactions, the background at high excitation energy is low compared to that in the stripping reactions, leading to the same final two nuclei. In the ^{91}Zr$(-n)$ reaction, the ground state (peak 0) is formed by the pickup of the outmost neutron in the $2d_{5/2}$ level with no ejectile excitation, and is shifted by 4.2 MeV from the centroid of peak 1. The ^{208}Pb ground state, seen in the ^{209}Bi$(-p)$ reaction, is obtained by the pickup of the outmost proton in the $1h_{9/2}$ level, and is shifted by 5.0 MeV from the centroid of the strongly excited peak 1.

The spectra from the same reaction on neighboring targets are again very similar. Deviations in reaction Q values of corresponding states for the reactions ^{90}Zr, ^{91}Zr, and ^{89}Y$(-n)$ were at most about 0.5 MeV. However, as seen in Table III, the excitation energies for states in the final nucleus ^{90}Zr are shifted by from 4.2 to 5.3 MeV compared to the corresponding states in the two neighboring nuclei.

The results, displayed in Table III, for peaks 1 and 2 in the reactions ^{208}Pb, ^{209}Bi, and ^{207}Pb$(-p)$, are consistent with the previous three cases. Q-value differences are less than 0.3 MeV, and the two excited states (peaks 1 and 2) of the final nucleus ^{208}Pb are shifted to higher

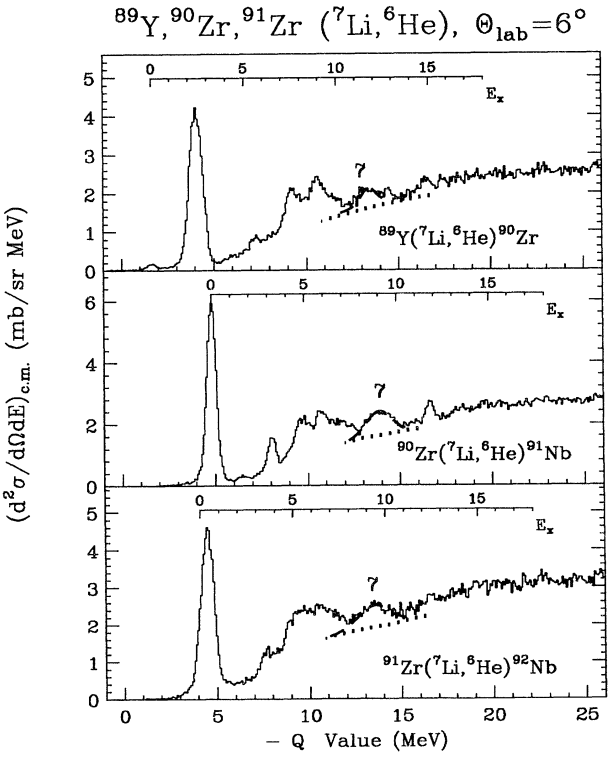

FIG. 3. Proton transfer spectra in the ^{90}Zr region from stripping reactions. The dashed lines are the fitted curves to the experimental results for the broad peaks (peak 7), and the dotted lines indicate the background assumed. Spectra are compared as a function of reaction Q value. The excitation energy scale is also given on each graph.

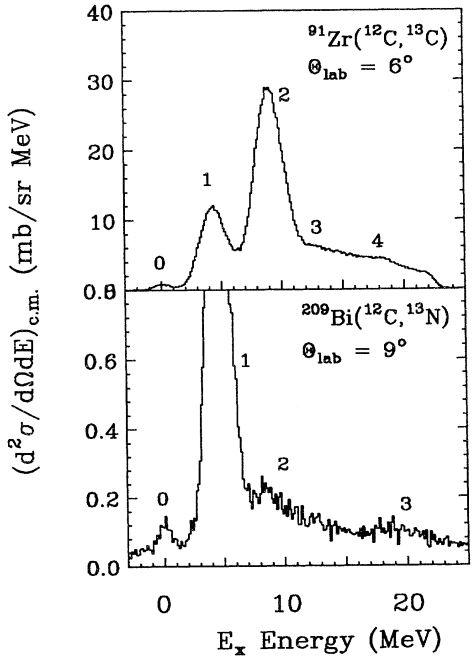

FIG. 4. Energy spectra of ^{91}Zr(^{12}C,^{13}C) and ^{209}Bi(^{12}C,^{13}N) reactions ($E_{\rm inc}$ = 30 MeV/nucleon) which lead to nuclei with closed shells in the ground state (peak 0).

excitation than the excited states of ^{206}Tl and ^{207}Tl by 2.1 and 3.6 MeV, respectively. However, the comparison for peak 3 suggests a different result. The reaction Q values of the centroids of peak 3 in the (^{12}C,^{13}N) reactions are 23.6, 20.4, and 23.5 MeV for final nuclei ^{207}Tl, ^{208}Pb, and ^{206}Tl. The corresponding excitation energies are 17.5, 18.5, and 18.0 MeV. In addition, the cross section of these states differ by a factor of 2 and the width of this peak is very large. This implies that perhaps this peak has a collective component which is excited to some significant degree.

B. Final nucleus has two particles or holes in the same orbit

In four of the reactions studied the ground state of the final nucleus has either two particles or holes in the same orbit: two neutrons from the neutron stripping reaction ^{91}Zr(^{7}Li,^{6}Li)^{92}Zr, two protons from the proton stripping reaction ^{209}Bi(^{7}Li,^{6}He)^{210}Po, two proton holes from the proton pickup reaction ^{89}Y(^{12}C,^{13}N)^{88}Sr, and two neutron holes from the neutron pickup reaction ^{207}Pb(^{12}C,^{13}C)^{206}Pb.

Energy spectra of the stripping reactions ^{91}Zr($+n$) and ^{209}Bi($+p$) are shown in Fig. 5. As was seen in the previous projectile stripping spectra, the background at high excitation is substantial and the ground states (labeled as peak number 0) are very weak. The $(2j_f+1)$ dependence of stripping reactions is a probable explanation for the weak ground state population of ^{92}Zr and ^{210}Po, which

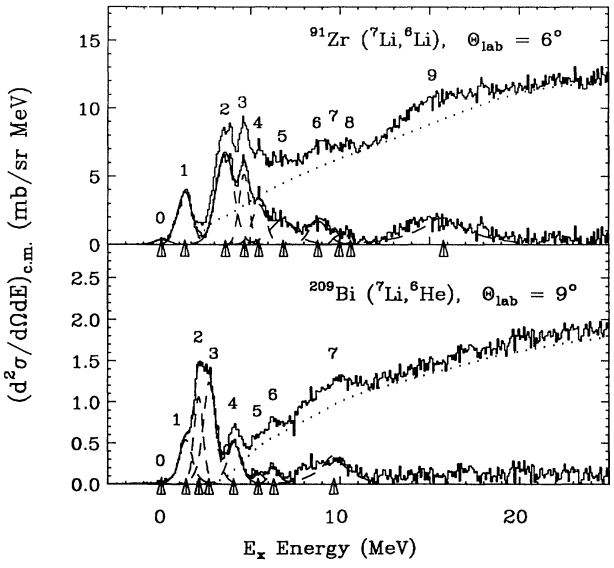

FIG. 5. Energy spectra of the ^{91}Y(^{7}Li,^{6}Li) and ^{209}Bi(^{7}Li,^{6}He) reactions (E_{inc} = 30 MeV/nucleon) which lead to nuclei with two particles in the same shells in the ground state (peak 0). The dotted lines indicate the background, and the underlying spectra are obtained after the background is subtracted. Arrows at the bottom in each spectrum represent the centroid of the peaks.

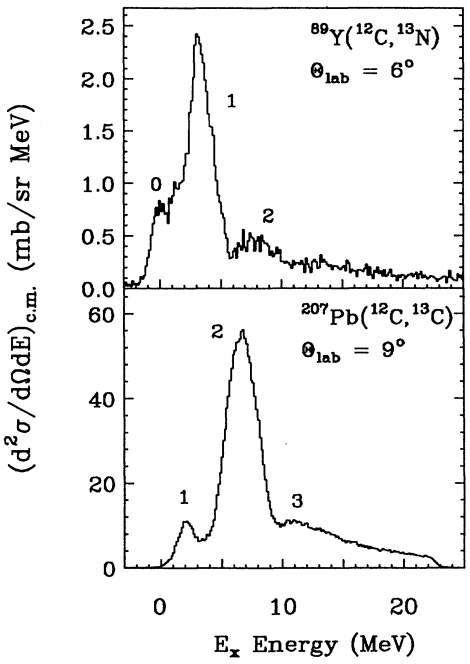

FIG. 6. Energy spectra of the ^{89}Y(^{12}C,^{13}N) and ^{207}Pb(^{12}C,^{13}C) reactions (E_{inc} = 30 MeV/nucleon) which lead to nuclei with two holes in the same shells in the ground state (peak 0).

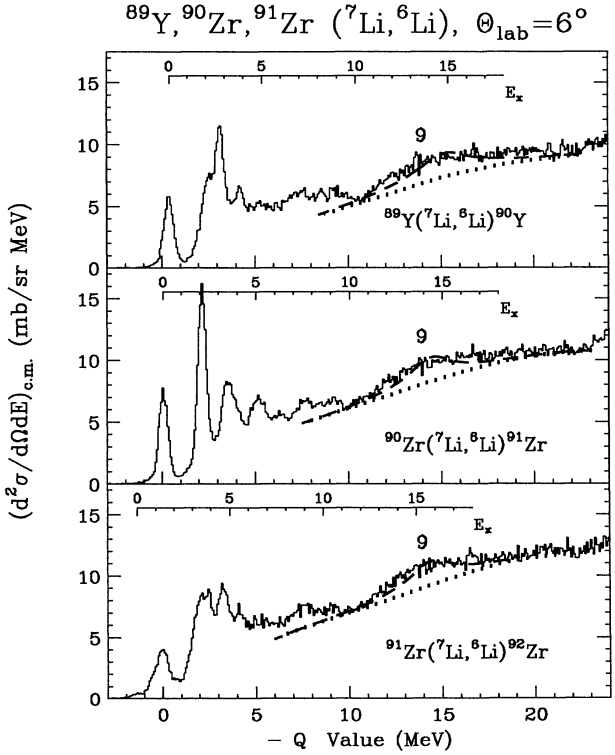

FIG. 7. Neutron transfer spectra in the ^{90}Zr region from stripping reactions (E_{inc} = 30 MeV/nucleon). The dashed lines are the fitted curves to the experimental results for the broad peaks (peak 9), and the dotted lines indicate the background assumed. Spectra are compared as a function of reaction Q value. The excitation energy scale is also given on each graph.

both have $j^\pi = 0^+$ ground states.

In the ^{91}Zr$(+n)$ reaction, nine excited states were analyzed including a broad peak (peak 9) at 15.8 MeV. The ^{91}Zr$(+n)$ spectrum is similar to the spectrum of ^{90}Zr$(+n)$ except that the relative strengths of peaks are changed slightly due to the coupling of single-particle states with the target's $1d_{5/2}$ state [20]. In the ^{209}Bi$(+p)$ reaction, seven excited states were analyzed including a broad state (peak 7) at 9.7 MeV. There is no significant difference at high excitation or at low excitation between the ^{209}Bi$(+p)$ spectrum shown in Fig. 5 and the ^{208}Pb$(+p)$ spectrum. The extra proton in the $1h_{9/2}$ level makes little difference to the relative strength of the peaks in the two spectra.

Energy spectra of the projectile pickup reactions ^{89}Y$(-p)$ and ^{207}Pb$(-n)$ are shown in Fig. 6. As was seen in the previous projectile pickup spectra, the background at high excitation energy is low, but the energy resolution is poor. The ground state of ^{88}Y is formed by pickup of a $2p_{1/2}$ proton in the ^{89}Y target. The ground state of ^{206}Pb is not seen in the ^{207}Pb$(-n)$ reaction due to the small value of $(2j+1)$ and large angular momentum mismatch.

For both the stripping and pickup cases the spectra of the same reactions on neighboring targets were com-

TABLE IV. Excitation energies for the strong, resolved peaks for pickup and stripping reactions on target sets of ^{90}Zr, ^{91}Zr, and ^{89}Y, and ^{208}Pb, ^{209}Bi, and ^{207}Pb. In each set one reaction leads to a nucleus with two particles or two holes in the same shell in the ground state and these reactions are marked by a *. Γ is a full width at half maximum, Q is the reaction Q value for a corresponding excitation energy, and the units are MeV. The uncertainty is about 0.15 MeV for ^{6}Li and ^{6}He, and about 0.3 MeV for ^{13}C and ^{13}N. Peak 0 is the ground state which is shifted to lower energy due to the particle-particle or particle-hole interaction.

	^{90}Zr(^{7}Li,^{6}Li)^{91}Zr			^{91}Zr(^{7}Li,^{6}Li)^{92}Zr *			^{89}Y(^{7}Li,^{6}Li)^{90}Y		
Peak	E_x	Γ	$-Q$	E_x	Γ	$-Q$	E_x	Γ	$-Q$
0				0.0	0.6	−1.4			
1	0.0	0.7	0.1	1.3	0.9	−0.1	0.1	0.7	0.5
2	2.1	1.0	2.2	3.6	1.2	2.2	2.2	1.1	2.6
3	3.6	1.0	3.7	4.7	0.9	3.3	2.8	0.8	3.2
4	5.1	1.0	5.2	5.5	1.0	4.1	3.7	1.1	4.1
5	6.3	1.2	6.4	6.8	1.6	5.4	4.9	1.6	5.3
9	14.4	6.0	14.5	15.8	6.0	14.4	14.0	6.0	14.4

	^{208}Pb(^{7}Li,^{6}He)^{209}Bi			^{209}Bi(^{7}Li,^{6}He)^{210}Po *			^{207}Pb(^{7}Li,^{6}He)^{208}Bi		
Peak	E_x	Γ	$-Q$	E_x	Γ	$-Q$	E_x	Γ	$-Q$
0				0.0	0.3	5.0			
1	0.0	0.8	6.2	1.4	0.8	6.4	0.0	0.9	6.3
2	0.7	0.6	6.9	2.1	0.7	7.1	0.9	0.9	7.2
3	1.4	0.7	7.6	2.7	0.7	7.7	1.5	0.6	7.8
4	2.6	0.8	8.8	4.1	1.0	9.1	2.7	1.0	9.0
7	8.4	4.0	14.6	9.7	4.0	14.7	8.4	4.0	14.7

	^{90}Zr(^{12}C,^{13}N)^{89}Y			^{91}Zr(^{12}C,^{13}N)^{90}Y			^{89}Y(^{12}C,^{13}N)^{88}Sr *		
Peak	E_x	Γ	$-Q$	E_x	Γ	$-Q$	E_x	Γ	$-Q$
0	0.0	1.5	6.4	0.0	1.5	6.7	0.0	2.0	5.1
1	1.6	3.0	8.0	1.9	3.0	8.6	3.0	3.0	8.4
2	6.6	6.0	13.0	6.1	6.0	12.8	7.9	5.0	13.0

	^{208}Pb(^{12}C,^{13}C)^{207}Pb			^{209}Bi(^{12}C,^{13}C)^{208}Bi			^{207}Pb(^{12}C,^{13}C)^{206}Pb *		
Peak	E_x	Γ	$-Q$	E_x	Γ	$-Q$	E_x	Γ	$-Q$
1	1.1	1.7	3.6	1.1	1.7	3.6	2.2	1.7	4.0
2	5.8	3.5	8.3	5.7	3.5	8.2	6.8	3.5	8.6
3	10.1	2.0	12.5	10.1	2.0	12.6	11.0	2.0	12.8

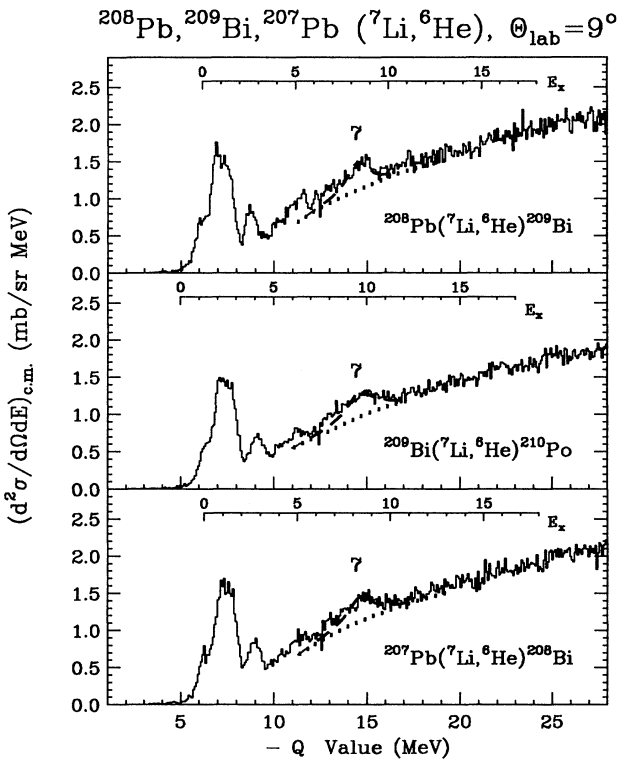

FIG. 8. Proton transfer spectra on ^{208}Pb region by stripping reactions ($E_{\rm inc}$ = 30 MeV/nucleon). The dashed lines are the fitted curves to the experimental results for the broad peaks (peak 7), and the dotted lines indicate the background assumed. Spectra are compared as a function of reaction Q value. The excitation energy scale is also given on each graph.

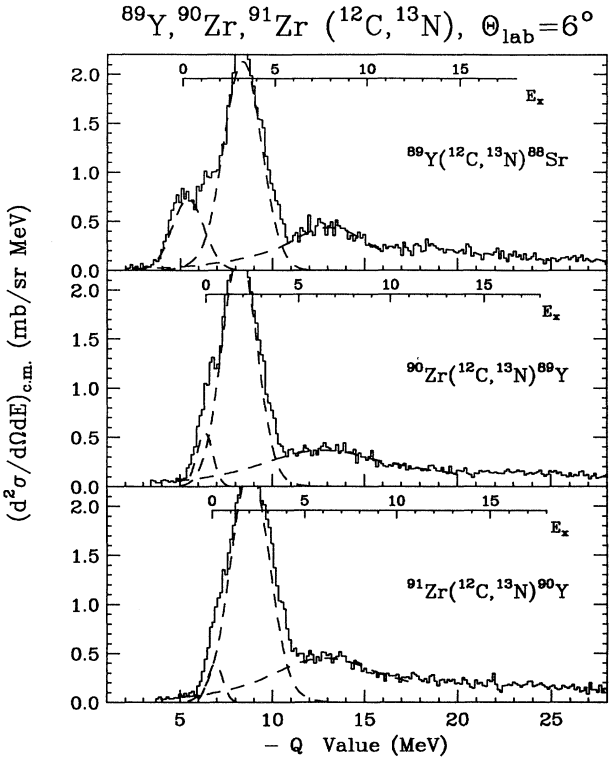

FIG. 9. Proton transfer spectra in the ^{90}Zr region from pickup reactions ($E_{\rm inc}$ = 30 MeV/nucleon). The dashed lines in each spectrum represent the fits to the experimental data using a Gaussian peak shape.

pared. Measured excitation energies, widths, and reaction Q values of the analyzed peaks and the broad peak in high excitation, identified in each spectrum are given in Table IV. The table includes four sets of three reactions, with each set containing one of the reactions that results in a final nucleus with two holes or particles in the same shell in the ground state.

For the set of reactions ^{90}Zr, ^{91}Zr, and ^{89}Y ($+n$), shown in Fig. 7, Q-value differences for corresponding states are less than 0.5 MeV, except for peaks 4 and 5, which were poorly resolved in the experiment. The excitation energy of states in the final nucleus ^{92}Zr with two neutrons in the outermost orbit is shifted to higher energy by 1.2–2.0 MeV. Reaction Q values for the peaks analyzed in the ^{208}Pb, ^{209}Bi, and ^{207}Pb ($+p$) reactions, shown in Fig. 8, are all within 0.3 MeV, while the excitation energy of states in the final nucleus ^{210}Po with two protons in the same orbit is shifted to higher energy by 1.1–1.5 MeV. Two neutrons in the same shell give very similar results to two protons in the same shell, as seen in the ^{91}Zr(^{7}Li,^{6}Li)^{92}Zr and ^{209}Bi(^{7}Li,^{6}He)^{210}Po reactions. Shell model calculations for two neutrons in the $2d_{5/2}$ state predict a shift of the ground state to lower energy by 1.26 MeV [21], and a similar shift to lower energy by 1.48 MeV for two protons in the $1h_{9/2}$ state [20]. The results of this experiment agree very well with these predictions.

The spectra for the (^{12}C,^{13}N) reaction on the set of neighboring targets ^{90}Zr, ^{91}Zr, and ^{89}Y are shown in Fig. 9. The data are plotted as a function of both the Q value and excitation energy. Figure 9 and Table IV show that the Q values of the two excited states identified are all within 0.5 MeV, while the excitation energy of these two states in the final nucleus ^{88}Sr with two proton holes is shifted to higher energy by 1.4–1.8 MeV. Peak 2 of the ^{89}Y(^{12}C,^{13}N)^{88}Sr spectrum, which has an excitation energy of 7.9 MeV, appears to be slightly narrower than those from the other two targets, while the total cross sections for peak 2 are nearly the same in all three reactions. A state corresponding to peak 2 was seen in a previous study, in which the authors designated it as a "giant resonancelike peak" [22]. However, the comparisons of the reaction Q values and excitation energies in the present work shows that the broad peaks labeled 2 have the characteristics of single-hole states rather than giant resonance states.

The results, displayed in Table IV, of the final reaction set ^{208}Pb, ^{209}Bi, and ^{207}Pb($-n$) are consistent with all previous cases. Q-value differences are less than 0.4 MeV, and for the reaction leading to the final nucleus ^{206}Pb with two neutron holes the spectrum is shifted to higher energy by about 1 MeV.

VI. CONCLUSIONS

Eight sets of neutron and proton, stripping and pickup reactions on lead and zirconium region targets were used to examine broad states at excitation energies close to those of giant quadrupole resonances, as well as low-lying states. The shell model predicts that single-particle states are shifted to higher excitation energies when the ground state of the final nucleus has a closed shell or two identical particles in the same orbit, and that the strength of corresponding states should be very similar for the same reaction on targets in the same mass region. If, however, the broad states are giant resonances formed by collective excitations, then the excitation energies of corresponding states in neighboring nuclei should vary smoothly and only to a small degree, while the cross section should be sensitive to the structure of the target.

Shell model calculations carried out on lead region nuclei predicted that the single-particle states, split into multiplets by an extra particle or hole in the target, are spread over 4 MeV. In this study the comparison of the shell model with experimental results agreed within a few hundred keV, and showed that the existence of an extra particle or hole outside a closed shell does not change the excitation energies significantly depending on the nuclear structure of the target ground state.

Only one set of broad peaks in the reactions examined in this experiment exhibited giant resonance features. They were observed at about 18 MeV in the proton pickup reaction (^{12}C,^{13}N) on lead region targets. These peaks have similar excitation energies but different Q values, different strengths, and were the widest peaks seen in the present study. In all other cases, high-lying broad peaks, like the low-lying states, are shifted to higher excitation energy when the ground state of the final nucleus has a closed shell or two identical particles in the same orbit. The observed shifts ranged from about 1.0 MeV for neutron pickup in the lead region to over 5 MeV for neutron pickup in the zirconium region. In addition, little variation in the strength of corresponding states was observed. These results lead to the conclusion that, with the exception of one set of states, the broad peaks formed in these reactions are due to the excitation of single-particle states rather than resulting from collective excitations.

This work was supported in part by the U.S. NSF under Grant No. PHY89-13815 and the Centre National de la Recherche Scientifique (CNRS, France).

[1] S. Gales, Ch. Stoyanov, and A. I. Vdovin, Phys. Rep. **166**, 125 (1988).
[2] S. Fortier, S. Gales, S. M. Austin, W. Benenson, G. M. Crawley, C. Djalali, J. S. Winfield, and G. Yoo, Phys. Rev. C **41**, 2689 (1990).
[3] Ph. Chomaz, N. Frascaria, S. Fortier, S. Gales, J. P. Garron, H. Laurent, I. Lhenry, J. C. Roynette, J. A. Scarpaci, T. Suomijarvi, N. Alamanos, A. Gillibert, G. Crawley, J. Finck, G. Yoo, and A. Van Der Woude, IPN Orsay, Annual Report No. 63, 1990.
[4] I. Lhenry, T. Suomijarvi, Y. Blumenfeld, Ph. Chomaz, N. Frascaria, J. P. Garron, J. C. Roynette, J. A. Scarpaci, D. Beaumel, S. Fortier, S. Gales, H. Laurent, A. Gillibert, G. Crawley, J. Finck, G. Yoo, and J. Barreto, in Proceedings of the Fourth International Conference on Nuclelus-Nucleus Collisions, Kanazawa, Report No. RIKEN-AF-105, 1991, p. 317.
[5] I. Lhenry, Ph.D. thesis, University de Paris XI, Orsay, 1992 (unpublished).
[6] S. Gales, C. P. Massolo, S. Fortier, E. Gerlic, J. Guillot, E. Hourani, J. M. Maison, J. P. Shapira, and B. Zwieglinski, Phys. Rev. Lett. **48**, 1593 (1982).
[7] C. P. Massolo, F. Azaiez, S. Gales, S. Fortier, E. Gerlic, J. Guillot, E. Hourani, and J. M. Maison, Phys. Rev. C **34**, 1256 (1986).
[8] Ph. Chomaz, J. Phys. (Paris) Colloq. **47**, C4-155 (1986).
[9] W. A. Lanford and G. M. Crawley, Phys. Rev. C **9**, 646 (1974).
[10] G. M. Crawley, E. Kashy, W. Lanford, and H. G. Blosser, Phys. Rev. C **8**, 2477 (1973).
[11] A. Bohr and B. R. Mottelson, *Nuclear Structure* (Benjamin, New York, 1969), Vol. 1.
[12] B. M. Sherrill, Ph.D. thesis, Michigan State University, 1985 (unpublished).
[13] Chin W. Ma and William W. True, Phys. Rev. C **8**, 2313 (1973).
[14] G. H. Herling and T. T. S. Kuo, Nucl. Phys. **A181**, 113 (1972).
[15] J. B. McGrory and T. T. S. Kuo, Nucl. Phys. **A247**, 283 (1975).
[16] E. K. Warbuton and B. A. Brown, Phys. Rev. C **43**, 602 (1991).
[17] B. A. Brown, A. Etchegoyen, and W. D. M. Rae, MSU NSCL Report No. 524, 1988.
[18] D. M. Brink, Phys. Lett. **40B**, 37 (1972).
[19] M. C. Mermaz, E. Tomasi-Gustafsson, B. Berthier, R. Lucas, J. Gastebois, A. Gillibert, A. Miczaika, A. Boucenna, L. Kraus, I. Linck, B. Lott, R. Rebmeister, N. Schulz, J. C. Sens, and C. Grunberg, Phys. Rev. C **37**, 1942 (1988).
[20] G. Yoo, Ph.D. thesis, Michigan State University, 1992 (unpublished).
[21] S. S. Ipson, K. C. McLean, W. Booth, and J. G. B. Haigh, Nucl. Phys. **A253**, 189 (1975).
[22] A. Stuirbrink, G. J. Wagner, K. T. Knopfle, Liu Ken Pao, G. Mairle, H. Riedesel, K. Schindler, V. Bechtold, and L. Friedrich, Z. Phys. A **297**, 307 (1980).